Hector: a new multi-object integral field spectrograph instrument for the Anglo-Australian Telescope

Julia Bryant, Joss Bland-Hawthorn, Jon Lawrence, Barnaby Norris, Seong-Sik Min, et al.

Julia J. Bryant, Joss Bland-Hawthorn, Jon Lawrence, Barnaby Norris, Seong-Sik Min, Rebecca Brown, Adeline Wang, Gurashish Singh Bhatia, Will Saunders, Robert Content, Ross Zhelem, Sudharshan Venkatesan, Mahesh Mohanan, Peter Gillingham, Robert Patterson, David Robertson, Naveen Pai, Helen McGregor, Jessica Zheng, Sam Vaughan, Caroline Foster, Sergio Leon-Saval, Scott Croom, "Hector: a new multi-object integral field spectrograph instrument for the Anglo-Australian Telescope," Proc. SPIE 11447, Ground-based and Airborne Instrumentation for Astronomy VIII, 1144715 (13 December 2020); doi: 10.1117/12.2560309

Event: SPIE Astronomical Telescopes + Instrumentation, 2020, Online Only

Hector - a new multi-object integral field spectrograph instrument for the Anglo-Australian Telescope

Julia J. Bryant[a,b], Joss Bland-Hawthorn[a,b], Jon Lawrence[c], Barnaby Norris[a], Seong-Sik Minh[a], Rebecca Brown[a,b,c], Adeline Wang[a,b,c], Gurashish Singh Bhatia[a], Will Saunders[c], Robert Content[c], Ross Zhelem[c], Sudharshan Venkatesan[c], Mahesh Mohanan[c], Peter Gillingham[c], Robert Patterson[c], David Robertson[c], Naveen Pai[c], Helen McGregor[c], Jessica Zheng[c], Sam Vaughan[a,b], Caroline Foster[a,b], Sergio Leon-Saval[a,b], Scott Croom[a,b]

[a] AAO-USydney, Sydney Institute for Astronomy (SIfA), School of Physics, The University of Sydney, NSW, Australia 2006;
[b] ARC Centre of Excellence for All Sky Astrophysics in 3 Dimensions (ASTRO 3D);
[c] AAO-MQ, Australian Astronomical Optics, Faculty of Science and Engineering, Macquarie University, NSW 2109, Australia;

Keywords: IFU, Hector, IFS, hexabundles, fibre positioner, AAT, spectroscopy

1. ABSTRACT

Based on the success of the SAMI integral field spectrograph (IFS) instrument on the Anglo-Australian Telescope (AAT), the capacity for large IFS nearby galaxy surveys on the AAT is being substantially expanded with a new instrument, Hector. The high fill-factor imaging fibre bundles 'hexabundles', of the type used on SAMI, are being improved and enlarged to cover 27-arcsec diameter. The aim is to reach 2 effective radii on most galaxies, where the galaxy rotation curve flattens and half of the angular momentum is accounted for. The boosted Hector spectral resolution of 1.3 Angstrom will enable higher order stellar kinematics to be measured on a larger fraction of galaxies than with any other IFS survey instrument.

Hector will have 21 hexabundles over a 2-degree field feeding both the new Hector spectrograph and existing AAOmega spectrograph. Hector consists of new blue and red-arm spectrographs, coupled to the new high-efficiency hexabundles and a unique robotic positioner. The novel robotic positioning concept will compensate for varying telecentricity over the 2-degree-field of the AAT to recoup the light loss and correct the focus across the field. The main components are in hand, and prototypes are currently being tested ahead of commissioning in the next year.

Hector will take integral field spectroscopy of 15,000 galaxies with $z < 0.1$ in the 4MOST WAVES-North and WAVES-South regions. The WAVES data, which will come later, will give the environment metrics necessary to relate how local and global environments influence galaxy growth through gas accretion, star formation and spins measured with Hector. The WALLABY ASKAP survey will trace HI gas across the Hector fields, which in combination with Hector will give a complete view of gas accretion and star formation.

2. INTRODUCTION

Multi-object integral-field spectrograph instruments such as SAMI[5,7] and MANGA[6] have undertaken resolved spectroscopic surveys of nearby galaxies. The SAMI survey completed 3000 galaxies, enabling ~ 50 refereed papers so far. Based on the success of SAMI we are building Hector (Bryant et al. in prep), the next main dark-time instrument for the 4m Anglo-Australian Telescope (AAT) near Coonabarabran in Australia. Hector will observe more galaxies at a time, have a larger 2-degree field of view, up to twice the coverage on each galaxy compared to SAMI and with the highest spectral resolution of any large IFS galaxy survey. Hector is enabled by optical fibre imaging bundles called *Hexabundles*[1–4], which have been improved and updated since those used in SAMI. It will have a new positioning system and a new higher-resolution spectrograph.

J.J.B.: E-mail: julia.bryant@sydney.edu.au

Ground-based and Airborne Instrumentation for Astronomy VIII, edited by Christopher J. Evans,
Julia J. Bryant, Kentaro Motohara, Proc. of SPIE Vol. 11447, 1144715 · © 2020
SPIE · CCC code: 0277-786X/20/$21 · doi: 10.1117/12.2560309

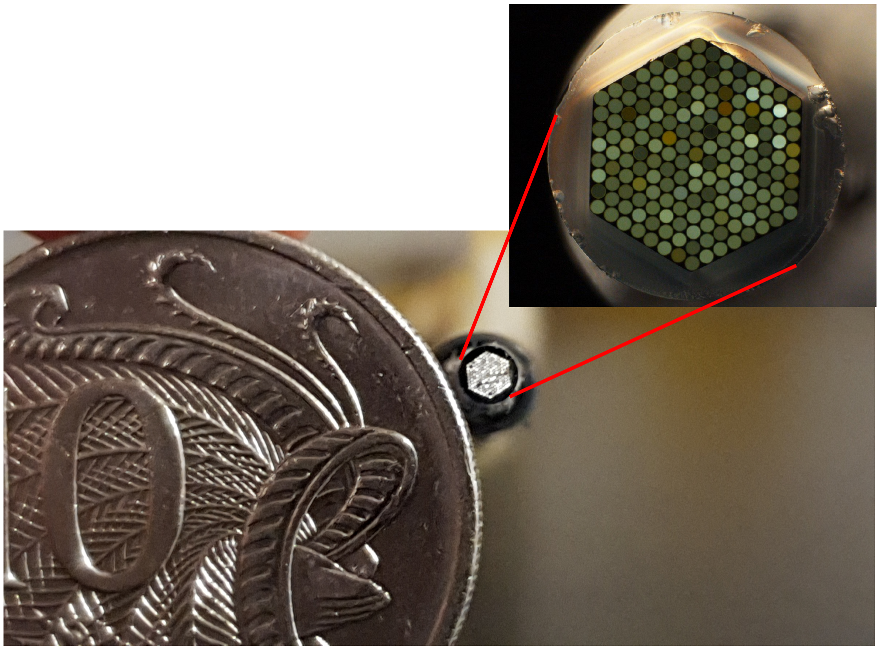

Figure 1. *One of the 169-core Hector hexabundles. Each fibre has a 103µm core. The optical diameter of this device is* $\sim 2mm$ *and is shown compared to an Australian 10 cent coin. The cores are randomly backlit.*

Hector is tailored to unique science that are unachievable with existing instruments. The Hector Galaxy Survey aims to observe 15,000 galaxies in sky regions overlapping substantial auxiliary data (in the GAMA[8] and 4MOST WAVES[*] regions). This statistical advantage enables the linking of galaxy structure and dynamics to galaxy environments. In particular, firstly, stellar kinematics will determine the merger history of galaxies matched to simulations. Secondly, measures of accretion and feedback across local to global environments will reveal the role of environment in controlling star formation across all galaxy types, and thirdly, galaxy spins compared to large-scale structure will disentangle the control of environment on galaxy growth.

3. HEXABUNDLES

Hexabundles were developed at the University of Sydney. Hexabundles on SAMI had twice the fill fraction (light collected within cores compared to lost between cores) than any other fibre IFUs due to the unique packing and fusing method. This method was carefully tailored to avoid the focal ratio degradation (FRD) that leads to light loss and is inherent in packing fibres together tightly.

19 new hexagonally-packed fibre bundles will image out to 2 effective radii in ∼70% of the galaxies in the Hector Galaxy Survey. Two further small hexabundles will observe standard stars. These new-generation hexabundles are being developed at the University of Sydney in the AAO-USydney node of the AAO. Five different sizes in hexabundles will contain 37-169 fibres per hexabundle, subtending between 15-26 arcsec on each galaxy. One of the 169-fibre hexabundles is shown in Figure 1.

Further details of the new Hector hexabundles and the focal ratio degradation testing of these devices can be found in the paper in these proceedings 11447-189 and in Wang et al. (in prep) and Brown et al. (in prep).

[*]https://wavesurvey.org/

4. POSITIONING SYSTEM

As Hector is being retrofitted to the AAT's 2-degree-field top end, all components have a very small space envelope to fit within. The hexabundle fibre ferules will lie across the 2-degree-field plate and have a prism assembly attached to the front face to redirect light into the fibres. The prisms are glued to the front face of each hexabundle and sky fibre. A magnetic system sets the tilt and rotation of each hexabundle in three axes to optimise field tiling configurations and to minimise loss by matching the telecentricity angle. Telecentricity changes inherent in the existing 2-degree field corrector mean the light is perpendicular to the plate in the centre but tilted by up to 4 degrees at the plate edge. This results in up to 20% light loss if the fibres are not tilted to match. The robotic system rotates tilted magnets to align the hexabundles with the telecentricity angle at all points across the field plate.

The magnet assembly relies on precision machined magnet casings (see Figure 2). The circular casings have four different highly accurate tilt angles, and the appropriate magnet is selected by the robot configuration software based on field radius. It is rotated and placed by the robot to align to the telecentricity tilt. A second high-precision rectangular magnet casing along the ferule will set the rotation angle of the ferule and provide support against torque or rotation of the hexabundle. A 'rotation arrestor' allows the ferules to tilt in 3 axes while maintaining connection with the second magnet. A third ring magnet is embedded in the prism holder to assist hexabundle attachment. The magnetic system allows for tilt and rotation in all three axes, is robust enough for manual changing of hexabundles between fields and at the same time gives enough force to withstand the gravitational changes from a required rotation of the top end up-side-down for observations. The magnetic casings have been designed to optimise the magnetic field strength in a small footprint by encasing the magnet in a *mirrax* casing. A precise gap between the internal magnet and the casing edges plus the casing design optimally directs the magnetic field lines down to the plate to increase the magnetic force by a factor of ~ 3 compared to bare magnets and at the same time constrains the field within the magnet casing to prevent interaction between closely-placed magnets.

A new positioning system consists of an Aerotech robot gantry (see Figure 2) that places locating magnets on a field plate off the telescope while the other plate is observing a field on-sky. The robot will be mounted on an optical bench located on the prime focus platform so the plates will be configured at the observing temperature. The observers will then lift the field plate, with its magnets attached, from the robot and mount the field plate in the 2dF top end and then manually attach the hexabundles and guide bundles to those locating magnets.

The magnet strength has been optimised to be sufficient to prevent them sliding or rotating as the telescope tilts or as the ferules are being fitted to the magnets, while having a force that is manageable by the robot (~ 80N). The design optimises the time taken for connecting and disconnecting hexabundles for field changes in order to improve survey efficiency.

4.1 Positioning System software

The Hector positioning system software consists of the following stages:

1. *Greedy tiling algorithm optimally selects galaxy tiles.* The regions of sky covered by the survey must have galaxies selected for each tile (see Figure 3 left) to minimise the number of tiles it takes to complete the galaxies in each region. Since galaxies are not evenly space, a greedy algorithm optimally "unpicks" the highest density regions first. This is essential in a few-pass survey in which each region of sky will be completed by only a few pointings (or field tiles) because the efficiency of the tiling is less for few-pass compared to multi-pass surveys. The density of galaxies in the survey is set by the Hector Galaxy Survey target selection criteria (Bryant et al. in prep) and the magnitude limit for the targets that can be observed with this instrument at this site.

2. *Position correction for thermal expansion and telecentricity offset.* Once the galaxy on-sky positions are determined for each field tile, they are translated into physical positions on the field plate. That transformation needs to account for optical distortions in the corrector, the thermal expansion of the field plate at the time it is configured compared to when it is observed, and the expansion of the robotic gantry as it positions. Additionally, the tilts of the components which correct for telecentricity also introduce a

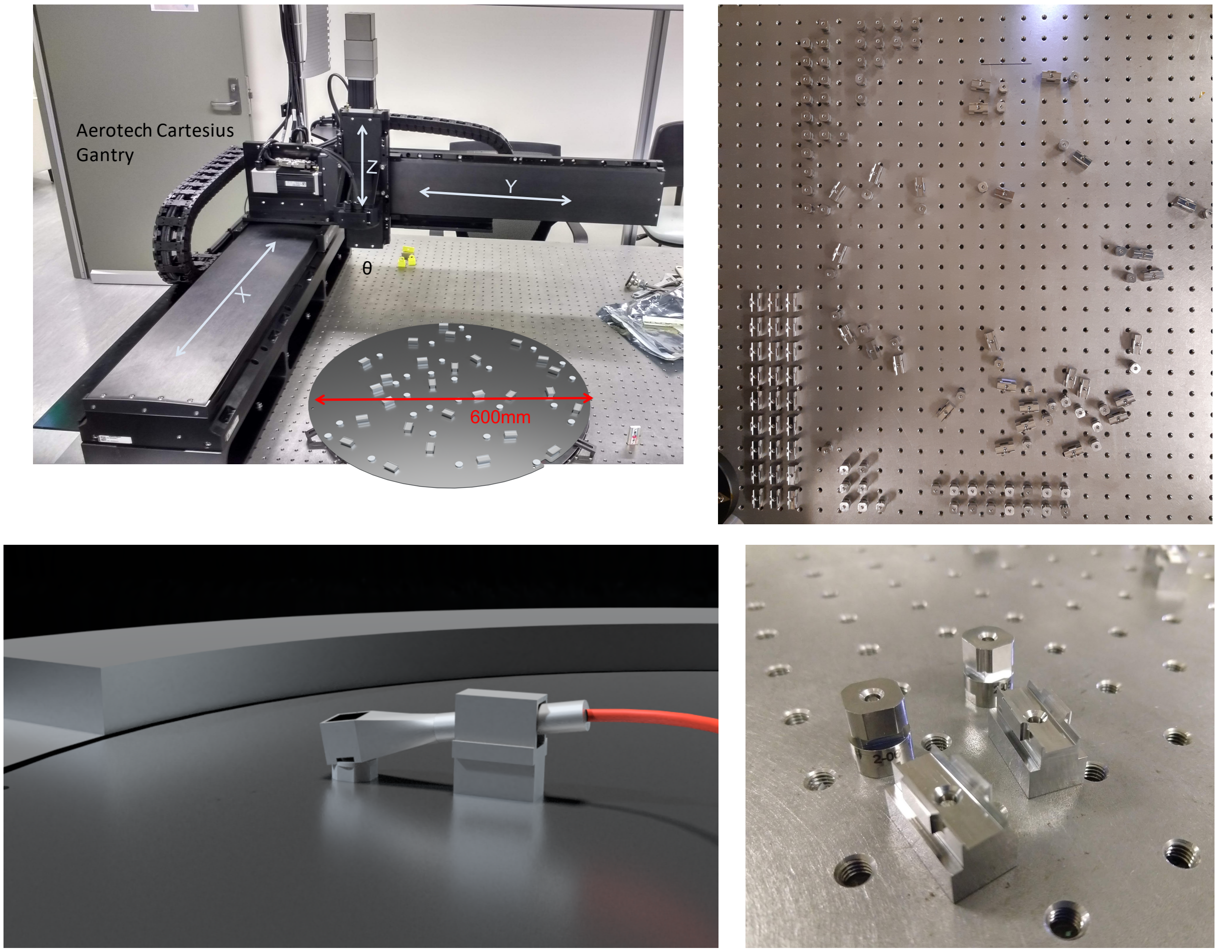

Figure 2. *Top left: The Hector x, y, z, θ robot gantry with a 600mm diameter 2-degree-field test plate with rendered magnet prototypes positioned that will hold the hexabundles. Top Right: The final manufactured high-precision magnet casings aligned on the optical bench by the robot positoner accurate to 10 microns. Some are in then holding positions and those in the centre are an actual configured science field. Note that this positioning is being tested directly on to an optical bench while the final invar plates and plate holder are being machined. Bottom left: Rendered image of the hexabundle ferule with rotation arrestor placed on the magnet pair. The tilt due to telecentricity is apparent and the rotation arrestor is designed to allow the ferule to tilt at any angle as the ferule is rotated around the tilted front circular magnet. The plate will hold 27 such assemblies. Bottom right: A close up of several of the high-precision magnet casings from the configuration above. The machining precision of the pick up edges on these casing and the tilts enables the pick up arm to hold and centre the casings to position them to within 10μm.*

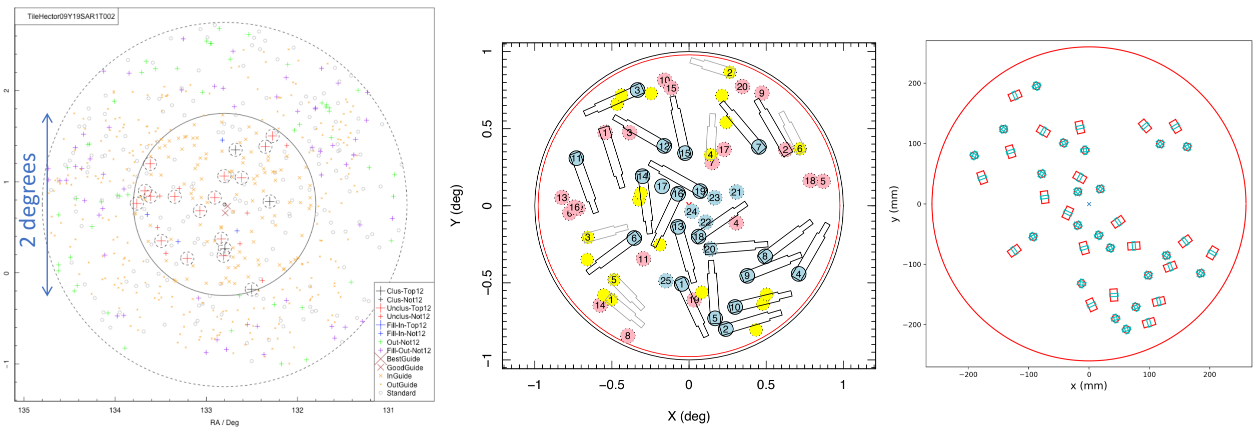

Figure 3. *Left: An example tile of one Hector field. Hector will observe many hundreds of such fields. This field shows the 2 degree on-sky region observed in the centre circle. The galaxies are "+" and those selected by the algorithm for this tiles are circled. The crosses and dots mark guide and standard stars respectively that are available in the region. 19 hexabundles will be allocated to galaxies, 2 to standard stars and 6 guide fibres will be on guide stars. Centre: An example field from the Configuration code. The blue circles mark the exclusion region around each galaxy (red and yellow for standard and guide stars) and the exclusion footprint required for each ferule is the black rectangle. The smaller stub rectangle at the end of each ferule is a clearance area to allow for the bend radius of the fibre cable coming out the back of the ferule. Right: The magnet positions matching this configuration, as found by the Collision code, for the circular and rectangular magnets.*

shift required for each magnet due to the geometrical shift of the top of the magnet and prism assembly compared to the base.

3. *Plate configuration to set ferule rotation.* Once the accurate physical positions of each galaxy are known, the Configuration code calculates the required rotation of the hexabundle ferule parallel to the field plate to enable all ferules to be positioned without collisions as shown in Figure 3(centre) . The code includes algorithms to optimise the ease with which the fibre cables will be able to navigate across the plate to one of three exit point from the field plate.

4. *Magnet placement order to prevent pickup arm collisions.* Once the configuration code has set the rotation, the circular magnet and rectangular magnet positions are then calculated to match the galaxy centre and the ferule rotation (see Figure 3 right) . The Collision code then considers the footprint of each magnet on the plate compared to the physical dimensions and movement of the robot pick up arm that will pick and place each magnet. The code determines if the pick up arm has sufficient clearance around each magnet to place it unobstructed. In crowded parts of the field that will not be the case and the code will resolve the direction and order for each magnet to be picked and placed to prevent collisions with the pick up arm.

5. *Labview control of the robot (including metrology).* A Labview interface reads in each of the tile files resulting from the culmination of the previous steps and controls the positioning by the robot gantry. It includes metrology that ensures the accuracy of placement of each part to within 10 microns. It has a recovery mode in case of power failure or human error, in which the code can recover an individual magnet and correct its placement rather than having to redo a full field. Each field takes approximately 55 mins to configure and another 55 minutes to unconfigure and return the magnets to their holding positions. This happens while the alternate field plate is on-sky observing and the observations are 3.5 hours, so there is not a tight time limit for the robot to configure the plate.

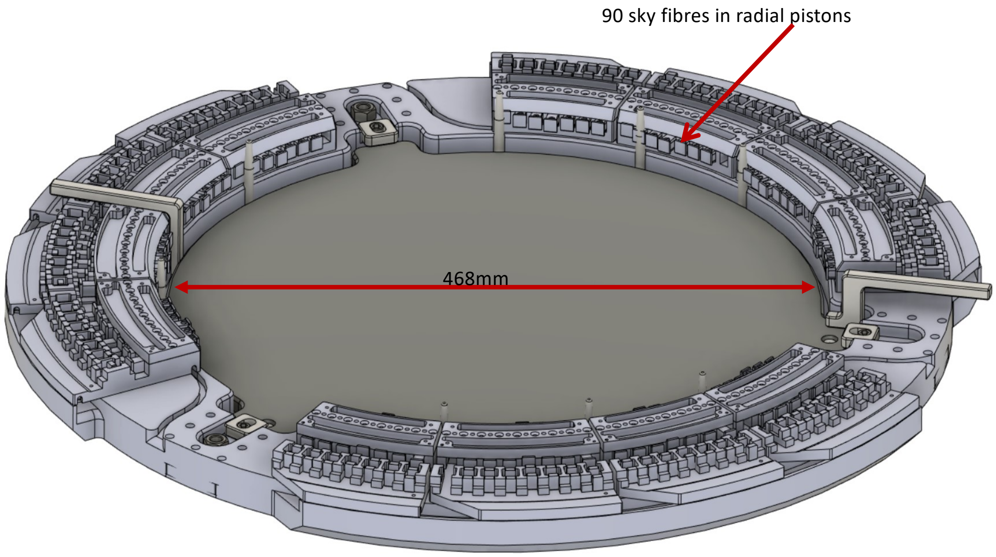

Figure 4. *Sky fibres lie radially around the outside of the field plate in 90 pistons. Pistons are arranged in 12 subplates that distribute the sky fibres feeding each of the two spectrographs semi-evenly around the field radius. Gaps between the sky fibre subplates enable the fibre cables from the hexabundles to exit the plate. Each piston can move inwards into the field to one of 3 positions to avoid contamination of the sky fibre.*

5. SKY FIBRE SYSTEM

Hector will have 90 sky fibres that are positioned around the outside perimeter of the field as shown in Figure 4. They are mounted in pistons that are positioned radially and allow the sky fibres to be located in one of 3 positions on-sky or in a blocked off position that receives no light. The sky fibre positioning software uses masks generated by PROFIT[9] to establish whether the sky fibre at each of those positions has any contamination from other sources on-sky. Position 1 is tested first and if clear, the sky fibres are left in that position by default. If contaminated then position 2 then 3 are checked. If all are contaminated then the sky fibre is moved to position 0 which is blocked off and it is not used for that observation.

The sky fibres on the field plate are mapped to the edge of each slitlet on the detector, with the science fibre from the hexabundles forming the centre fibres in each slitlet. Slitlets are lined up on the slit feeding into each spectrograph. On the detector there are gaps between each slitlet that allow background light and scattered light in the spectrograph to be fitted and removed during the data reduction. Since different sky fibres will be blocked off in each observation, the gaps between the slitlets will be wider or narrower in each image, but always maintaining the minimum number of clear pixels required to reach the background level once the wings of the adjacent science fibre PSFs are accounted for.

Full details of the sky fibre system can be found in the paper in these proceedings 11447-172 and in Bhatia et al. (in prep).

6. SPECTROGRAPHS

Two spectrographs will be fed by the Hector hexabundles - AAOmega and the first new Hector spectrograph. AAOmega is the AAT's work-horse spectrograph. It provides a flexible wavelength range of $375 - 575$ nm and

630 − 740 nm respectively in the red and blue arms, with a resolution ($\frac{\lambda}{d\lambda}$) of ∼ 1810 at 480 nm, and ∼ 4260 at 685 nm. The new Hector spectrograph is a dual arm, fixed resolution, dedicated spectrograph. It provides an instrumental spectral resolution of at least 0.13 nm from 372.7 − 776.1 nm with 2 pixel FWHM spectral sampling. In total 854 and 811 fibres will feed the Hector and AAOmega spectrographs respectively including hexabundle and sky fibres.

Further details of the new Hector spectrograph can be found in the paper in these proceedings 11447-198, 11447-200 and 11447-219.

7. CONCLUSION AND ACKNOWLEDGEMENTS

The Hector Galaxy Survey will begin in mid 2021 after commissioning of the Hector instrument in 2021A. New-generation larger hexabundle prototypes have been developed and are close to completing final production. The spectrograph design is complete and optics are in hand and being assembled, and the new positioning system is currently being tested with its final parts and components mostly delivered. The high spectral resolution will enable unique science with Hector that cannot be done by any other multi-object IFS survey. Hector aims to complete a survey of 15,000 galaxies at z<0.1 which will disentangle the influence of environment from the largest-scales to local halos, on the merger history and evolution of galaxies in the local Universe.

Parts of this research is supported by the Australian Research Council Centre of Excellence for All Sky Astrophysics in 3 Dimensions (ASTRO 3D), through project number CE170100013 and through ARC LIEF grants LE150100144, LE170100242, LE190100018. JJB acknowledges support from an ARC Future Fellowship FT180100231.

REFERENCES

1. Bland-Hawthorn J., et al., Optics Express, 19, 2649 (2011)
2. Bryant J. J., O'Byrne J. W., Bland-Hawthorn J., Leon-Saval S. G., MNRAS 415, 2173 (2011)
3. Bryant J. J., Bland-Hawthorn J., et al., Proc. SPIE 8446, 250 (2012)
4. Bryant J.J., Bland-Hawthorn J., Fogarty L., Lawrence J., Croom S., MNRAS, 438, 869, (2014)
5. Bryant J. J. et al., MNRAS, 447, 2857 (2015)
6. Bundy K. et al., ApJ, 798, 7 (2015)
7. Croom S., et al. MNRAS 421, 872 (2012)
8. Driver S.P., et al., A&G, 50, 12 (2009)
9. Robotham A. S. G., Taranu D. S., Tobar R., Moffett A., Driver S. P. , MNRAS 466,1513 (2017)